

Blue Quantum Dot Light-Emitting Diodes with High Electroluminescent Efficiency

Lishuang Wang,^{†,‡} Jie Lin,^{*,†,§} Yongsheng Hu,[†] Xiaoyang Guo,^{†,§} Ying Lv,^{†,§} Zhaobing Tang,^{†,‡} Jialong Zhao,^{*,§} Yi Fan,[†] Nan Zhang,[†] Yunjun Wang,^{||} and Xingyuan Liu^{*,†,§}

[†]State Key Laboratory of Luminescence and Applications, Changchun Institute of Optics, Fine Mechanics and Physics, Chinese Academy of Sciences, Changchun, 130033 Jilin, China

[‡]University of Chinese Academy of Sciences, Beijing 100049, China

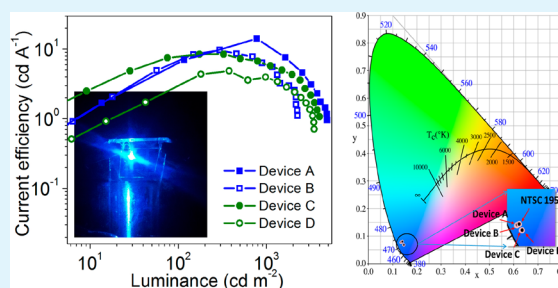
[§]Key Laboratory of Functional Materials Physics and Chemistry of the Ministry of Education, Jilin Normal University, Siping, 136000 Jilin, China

^{||}Suzhou Xingshuo Nanotech Co., Ltd. (Mesolight), Suzhou, 215123 Jiangsu, China

Supporting Information

ABSTRACT: High-efficiency blue CdSe/ZnS quantum dots (QDs) have been synthesized for display application with emission peak over 460 nm with the purpose of reducing the harmful effect of short-wavelength light to human eyes. To reach a better charge balance, different size ZnO nanoparticles (NPs) were synthesized and electrical properties of ZnO NPs were analyzed. Quantum dot light-emitting diodes (QLEDs) based on as-prepared blue QDs and optimized ZnO NPs have been successfully fabricated. Using small-size ZnO NPs, we have obtained a maximum current efficiency (CE) of 14.1 cd A⁻¹ and a maximum external quantum efficiency (EQE) of 19.8% for QLEDs with an electroluminescence (EL) peak at 468 nm. To the best of our knowledge, this EQE is the highest value in comparison to the previous reports. The CIE 1931 color coordinates (0.136, 0.078) of this device are quite close to the standard (0.14, 0.08) of National Television System Committee (NTSC) 1953. The color saturation blue QLEDs show great promise for use in next-generation full-color displays.

KEYWORDS: quantum dots, light-emitting diodes, EQE, CIE 1931 color coordinates, high efficiency



INTRODUCTION

Because of their excellent characteristics, such as high photoluminescence (PL) efficiency, high color saturation, solution-progress fabrication, and large-area production, quantum dot light-emitting diodes (QLEDs) have become one of the most interesting research hotspots in display fields during the past 30 years. Despite the fact that fast development and great enhancement in electroluminescence (EL) performance have been obtained for red and green QLEDs whose external quantum efficiencies (EQEs) reach up to 20.5 and 21%,^{1–3} respectively, the realization of high-efficiency blue QLEDs is still a serious need for next-generation solid-state lighting and displays.

In 2007, a pure blue EL was realized in the QLED based on core/shell CdS/ZnS nanocrystal quantum dots (QDs) that has a narrow spectrum full width at half-maximum (FWHM) of 20 nm.⁴ However, the 5.5 V turn-on voltage (V_{on}) was quite high, and deep reape emission was found in this device. To enhance the EL performance, optimized synthesis for high-quality QDs is one of the key factors. Blue QLEDs based on alloyed shell QDs,⁵ surface ligand-optimized QDs,⁶ size-tunable violet–blue (400–450 nm) QDs,⁷ and tailored nanostructure QDs⁸ were reported with good EL properties. A high current efficiency

(CE) of 4.4 cd A⁻¹ and EQE of 12.2% were achieved for QLEDs with an emission peak at 450 nm.⁶ Methods aimed at enhancing hole injection by gold nanoparticle-doped hole injection layer (HIL)⁹ and enhancing hole transportation by optimization of hole transport layer (HTL)¹⁰ were incorporated into the fabrication of QLEDs. A rather high EQE of 7.39% and luminance of 2856 cd m⁻² were achieved in the electrical modification device.¹⁰

While most reported QLEDs are ultraviolet–deep blue or blue colors,^{8,11–13} there are few studies that focus on blue QLEDs with an emission peak over 460 nm. As we know, a shorter emission peak corresponds to a greater light energy. For the purpose of lowering the influence of great energy on human eyes for display applications, it is significant to develop pure blue QLEDs whose Commission International de l'Éclairage (CIE) 1931 color coordinates should be close to the National Television System Committee (NTSC) 1953 standard. Recently, a high CE of 16.1 cd A⁻¹ for blue QLED was obtained by using a transparent indium tin oxide (ITO)/Ag/

Received: July 22, 2017

Accepted: October 17, 2017

Published: October 17, 2017

ITO electrode.¹⁴ However, the blue QLED was obtained with a FWHM of 35 nm corresponding to CIE 1931 color coordinates of (0.11, 0.13), which is far from that of NTSC 1953 standard. Herein, we used thick-shell CdSe/ZnS QDs, whose PL emission peak can be varied from 462 to 466 nm, as the emitting layer (EML) to adjust the CIE property.

EQE is a very important EL characteristic for QLEDs. The EQE is defined as the ratio of the number of photons emitted by the device to the number of electrons injected. To enhance the EQE, the internal quantum yield, especially the fraction of injected charges that form excitons, should be effectively improved. For QLEDs, high PL quantum yield (PL QY) could be achieved by optimized synthesis condition of QDs. Only if the energy level of each function layer for charge injection and transport is quite opposite can the fraction of injected charges that forms excitons be enhanced.

ZnO nanoparticles (NPs) can form films by spin-coating methods and have excellent electron transport property. QLEDs that used ZnO NPs as electron transport layer (ETL) and organic/polymer films as HTL have been one of the most promising developing tendencies.^{11,15} In this work, the influence of different size ZnO NPs with step-controlled mixing process on EL performance was investigated, and the energy level and mobility properties of ZnO NPs were analyzed. Herein, we report high-efficiency conventional organic–inorganic hybrid blue bottom-emission QLEDs by using thick outer shell CdSe/ZnS QDs as the EML and size-varied ZnO NPs layer as the ETL for a better charge balance. The used QDs have high PL QY due to a large limitation of nonradiative recombination progress by thick outer shells. An EL emission peak of 468 nm, a record EQE of 19.8%, and a maximum CE of 14.1 cd A⁻¹ were obtained for the best performing QLED. The CIE 1931 color coordinates (0.136, 0.078) of this device are quite close to the NTSC 1953 standard of (0.14, 0.08). The color saturation property makes this QLED an ideal blue light source for display application. Quite high EQE of 11.9% for 464 nm device was also obtained in this work with the optimized ETL.

RESULTS AND DISCUSSION

In general, photophysical properties of QDs play an important role in determining the EL performance of QLEDs. A powerful strategy for QD synthesis is covering the core with a thick shell, so that QDs can retain high PL QY and stability. The average size of QDs used here is 12–13 nm, which was determined by the transmission electron microscope (TEM) images of 462 and 466 nm QDs, as shown in Figures S1 and S2. It can be observed that the QDs exhibit good monodispersivity. Ultraviolet visible absorption (UV-abs) spectroscopy and PL spectra of QDs are illustrated in Figure 1a. The two blue CdSe/ZnS QDs show PL peaks at 462 and 466 nm and exhibit high PL QYs of 70% and 87%, respectively. The PL decay curves of QDs in solution and solid state are shown in Figure 1b. QDs in solution show a PL decay in a dual-channel form. The excited-state lifetime is decreased when QDs are changed from solution state to solid state. A lifetime reduction is observed in both 466 and 462 nm QD films (20 nm thick, on glass).

The thick-shell CdSe/ZnS QDs are chosen as the EML not only for their nearly identical PL properties but also for the minimized Auger recombination (AR) effect in such a nanostructure. The thick shell in QDs shows a physical barrier that can effectively reduce the Förster resonant energy transfer (FRET), which is sensitive to inter-QDs spacing.¹⁶ Incorporation

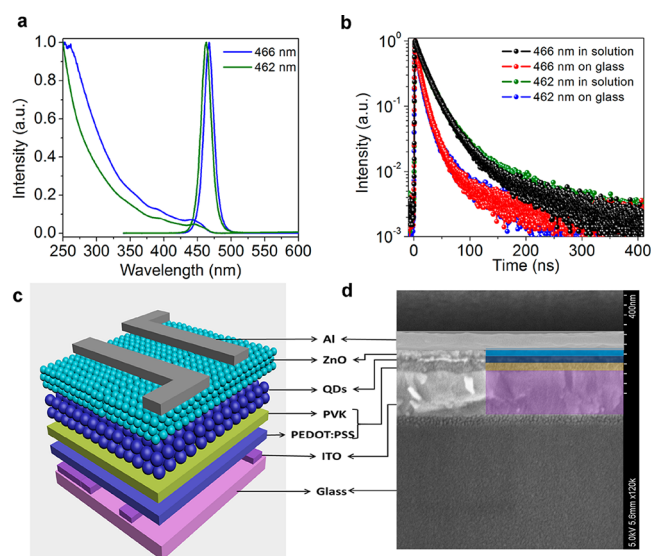


Figure 1. (a) UV-abs and PL spectra of QDs with different emission peaks. (b) PL decay curves of QDs in solution and solid state. (c) Structure mechanism diagram of QLED. (d) Cross-section SEM image of QLED.

of thick shell into QDs is demonstrated to limit nonradiative recombination progress effectively, resulting in an improved luminance and EQE in QLEDs.^{17,18} Fabrication of QLEDs was conducted based on optimized multilayer structure, which is shown in Figure 1c: ITO, poly(ethylenedioxythiophene):polystyrene sulfonate (PEDOT:PSS, 20 nm), poly(9-vinylcarbazole) (PVK, 30 nm), QDs (20 nm), ZnO NPs (30 nm), and aluminum (Al, 100 nm) were used as anode, HIL, HTL, EML, ETL, and cathode, respectively. The cross-section scanning electron microscope (SEM) image in Figure 1d shows that the interfaces of the multiple layers are in distant contact.

Most of the synthesis of ZnO NPs begins with a certain molecular proportion of [Zn]²⁺/[OH]⁻, such as the doping ZnO NP.^{19,20} In the work, it is found that the controlled mixing progress of [Zn]²⁺/[OH]⁻ plays a certain role in determining the property of ZnO NPs. The detailed synthesis of ZnO NPs is provided in the experimental section (Supporting Information). Allowing for the different dropwise speed of potassium hydroxide, the concentration of [OH]⁻ has a significant influence on the particle size. A higher concentration of [OH]⁻ leads to a bigger particle size of ZnO NPs, which is in line with the previously reported tendency.²¹ As illustrated in surface morphology images (Figure 2a and b), the particle size of ZnO NPs A is smaller than that of ZnO NPs B, and the surface roughness of ZnO NPs B (3.888 nm) is larger than that of ZnO NPs A (3.626 nm). The X-ray diffraction (XRD) patterns of the ZnO NPs together with bulk phase ZnO are shown in Figure S3. Comparison of the diffraction peaks suggests that the as-prepared ZnO NPs are crystalline and assigned to the hexagonal zincite structure similar to that of bulk ZnO. The PL spectra of ZnO NPs in Figure 2c shows a wide trap-state emission from 450 to 650 nm. The PL peak intensity of ZnO NPs A is much higher than that of ZnO NPs B, so it is inferred that ZnO NPs A layer has more trap states. Under the excitation wavelength of 320 nm and the same experimental condition, PL spectra of ZnO NPs A and a structure of QDs/ZnO NPs A are compared in Figure S4. It can be observed that the PL intensity of ZnO NPs A is nearly 2

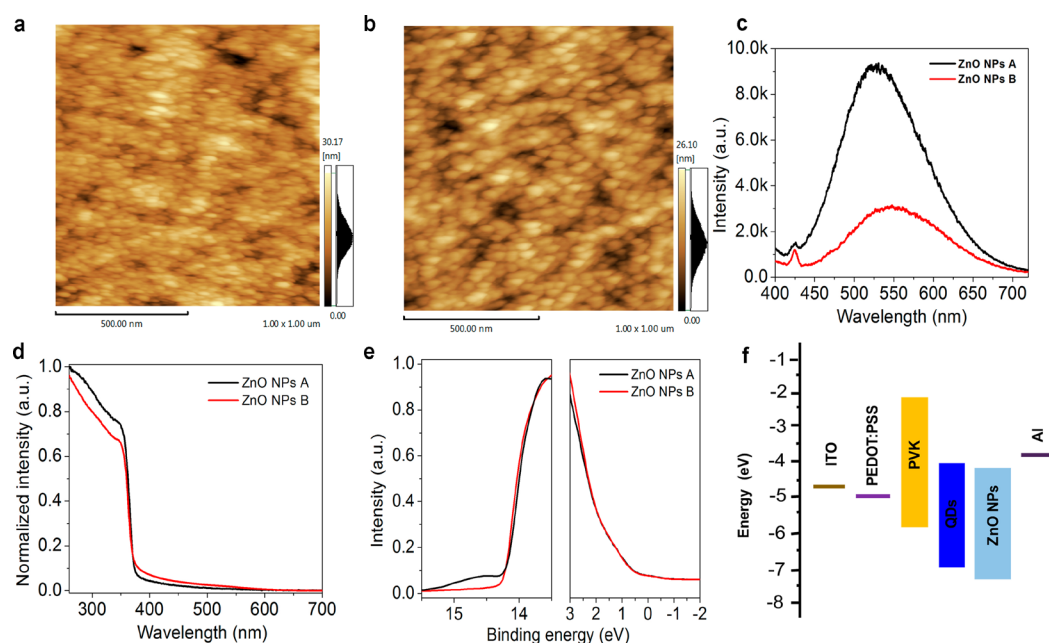


Figure 2. Surface morphology of ZnO NPs on glass: (a) ZnO NPs A and (b) ZnO NPs B. (c) PL spectra, (d) UV-abs spectroscopy, and (e) UPS spectra of different colloidal ZnO NPs. (f) Energy-level diagram of QLED.

orders of magnitude lower than that of QDs. Therefore, the PL spectra of QDs/ZnO NPs A show only the characteristics of QDs, which means that the PL intensity of ZnO NPs has a negligible effect on that of QDs. It is well-known that the conductivity and electron mobility would be enhanced with the decrease of the size of ZnO NPs. As shown in Figure S5, mobility of different colloidal ZnO NPs was achieved by fitting the space-charge-limited-current region with Child's law, and a higher electron mobility of $8.36 \times 10^{-4} \text{ cm}^2 \text{ V}^{-1} \text{ s}^{-1}$ was obtained for ZnO NPs A as expected.

To investigate the band gap and energy level of different colloidal ZnO NPs, the UV-abs spectroscopy and ultraviolet photoelectron spectroscopy (UPS) were measured and are shown in parts d and e of Figure 2, respectively. The band gaps of ZnO NPs A and B are 3.34 and 3.32 eV, respectively. As demonstrated in UPS spectra, the high-binding energy cutoff (E_{cutoff}) and the onset energy in valence-band edge (E_{onset}) regions change with the variation of ZnO particle size. The valence band maximum (VBM) is determined according to the equation of $\text{VBM} = 21.2 - (E_{\text{cutoff}} - E_{\text{onset}})$, which is -7.46 and -7.43 eV, respectively, for ZnO NPs A and B. The conduction band maximum (CBM) can be calculated based on the band gap and VBM, which is -4.12 and -4.11 eV for ZnO NPs A and B, respectively. With the suitable CBM of ZnO NPs, the electrons are facilitated to inject into the EML. Figure 2f shows the energy-level diagram of multiple layers in the QLED. In a conventional device with an organic–inorganic hybrid charge-transport layer, the carrier injection barrier at the HTL/EML interface is larger than that at the ETL/EML interface, which limits the hole injection into the QD layer. The unbalanced carrier injection can result in excess electrons in EML. Generally speaking, the excess electrons may cause many problems, for example, a reduction of the fraction of charges that form excitons, trion emission formed by charging QDs, or decrease of device lifetime.²² To improve device performance by decreasing the band offset between HTL and EML, the selection of HTLs with an appropriate highest occupied molecular orbital (HOMO) energy level is very important.

The PVK used in this work has the lowest HOMO of -5.8 eV (Figure S6) and is among the most widely used hole transport materials, such as poly(N,N' -bis(4-butylphenyl)- N,N' -bis(phenyl)benzidine) (poly-TPD, HOMO of -5.2 eV)²³ and poly[9,9-dioctylfluorene-*co*- N -[4-(3-methylpropyl)]-diphenylamine] (TFB, HOMO of -5.3 eV).²⁴ So, PVK is a rather ideal HTL material to lower the hole injection barrier at the HTL/EML interface, especially for blue QLEDs.

The current densities of electron-only devices with the structure of ITO/ZnO NPs/QDs/ZnO NPs/Al are shown in Figure 3a. These devices are device a with 466 nm QDs/ZnO

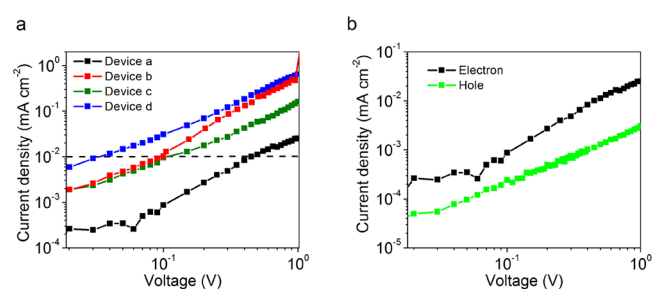


Figure 3. (a) Current density–voltage (J – V) curves of electron-only devices. (b) J – V curves of electron-only device a (black line) and hole-only device e (green line).

NPs A, device b with 466 nm QDs/ZnO NPs B, device c with 462 nm QDs/ZnO NPs A, and device d with 462 nm QDs/ZnO NPs B. Detailed thickness of multiple layers in electron-only and hole-only devices is shown in the Supporting Information. With the large-particle-size ZnO NPs B, the current density of electron-only device d is higher than that of device c, which is likely caused by a larger leakage current owing to the higher surface roughness of ZnO NPs B in consideration of the ZnO NPs/QDs/ZnO NPs sandwich structure in electron-only devices. Similar results were obtained for devices a and b. Current density of hole-only device e with the structure of ITO/PEDOT:PSS/PVK/466 nm QDs/

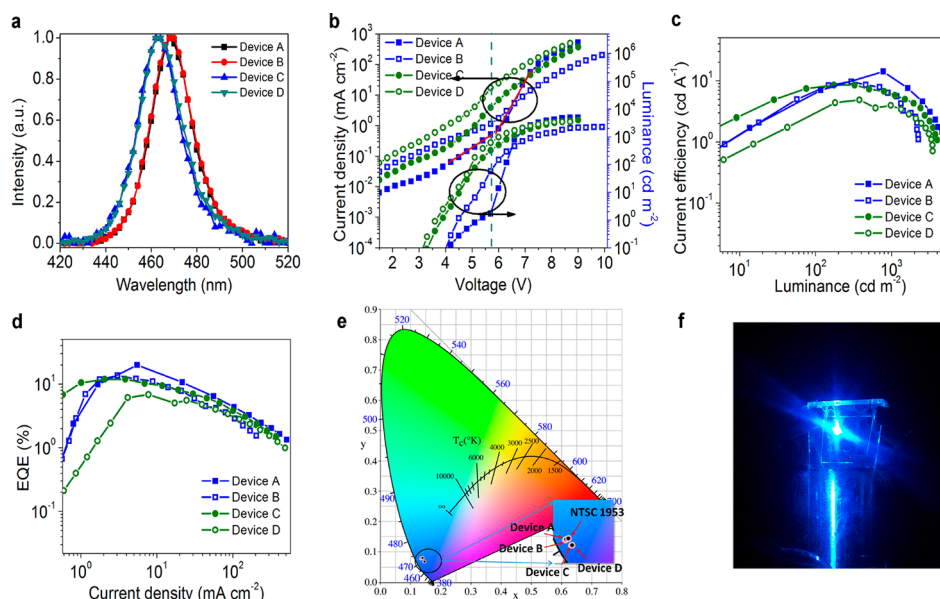


Figure 4. EL performances of QLEDs. (a) Normalized EL spectra. (b) Luminance–voltage–current density (L – V – J) characteristics of QLEDs. (c) CE properties as a function of luminance. (d) EQE properties as a function of current density. (e) CIE properties. (f) Image of device A at driving voltage of 7 V.

MoO₃(30 nm)/Al is demonstrated in Figure 3b. For 466 nm QDs, the average current density of electron-only device a is ~ 20 times higher than that of hole-only device e. The relatively close current density between electron-only and hole-only devices would be beneficial to reach a better charge balance as well as good EL performance in QLEDs.

EL performances of QLEDs are demonstrated in Figure 4. As normalized spectra presented in Figure 4a, the peak wavelengths are 464 nm for devices C and D and 468 nm for devices A and B. EL spectra have a 2 nm red-shift compared with that of PL spectra (Figure 1a), which is caused by the interdot interactions and the electric-field-induced Stark effect.²⁵ As shown in Figure 4b, the maximum luminance (L) of 4890 cd m⁻² was obtained at a driving voltage of 9 V for device A. A luminance inflection point occurs in device A at a driving voltage of 5.7 V (as shown by dark cyan line) with a luminance of 1.70 cd m⁻² due to the fluctuation in current density as illustrated in the fitted J – V curves (red line) of device A. At low driving voltage range, the current density of devices A and C is lower than their counterparts (devices B and D). Because ZnO NPs A and B have approximate band gap, CBM, and VBM, the major difference between them is that ZnO NPs A has a low surface roughness and more trap states than ZnO NPs B. Therefore, the observed J – V curves imply that the quality of interface contact and trap states may have a big influence on ZnO NPs/QDs interface barrier and subsequent electron injection. Figure 4b shows that the V_{on} at luminance of 1 cd m⁻² are 3.6, 3.9, 4.4, and 5.1 V for devices D–A, respectively. Devices A and B with 466 nm QDs have higher V_{on} than that of devices C and D with 462 nm QDs. It is known that both EML (QDs) and ETL (ZnO NPs) can influence the V_{on} of devices. The observed V_{on} difference suggests that, in addition to aforementioned interface contact and trap states, QDs with different shell thicknesses may have a nonnegligible effect on the V_{on} for blue QLEDs.

CE as a function of luminance and EQE as a function of current density are demonstrated in Figure 4c and d. A record maximum CE of 14.1 cd A⁻¹ is obtained at a luminance of 782

cd m⁻² for device A. As particle size of ZnO NPs increased, the maximum CE decreased to 9.69 cd A⁻¹ for device B. Using 462 nm QDs as the EML, the maximum CE of 8.48 cd A⁻¹ is achieved for device C. The CE reduction from devices A and C, which used the same ETL, is mainly caused by the PL QY decrease of QDs. As for the electron-only device described in Figure 3, a more balanceable charge injection was achieved for device A compared to other devices. The highest EQE of 19.8% was obtained at a current density of 5.53 mA cm⁻² for device A. To the best of our knowledge, it is the highest value as compared to the previous reports. The highest EQE can be attributed to the better charge balance in the device and the used high PL QY and thick-shell QDs that have suppressed the nonradiative process. A maximum EQE of 13.6% is reached for device B at a current density of 3.04 mA cm⁻². The maximum EQEs of devices C and D are 11.9% and 6.82%, respectively. There is obvious efficiency roll-off for blue QLEDs in this work, which originates mainly from reduced charge balance and all kinds of nonradiative exciton quenching processes such as nonradiative Auger processes, dissociation of excitons under high fields, and electric-field-induced decrease in PL efficiency of QD.^{26,27} It has been reported that the field-induced PL decrease is more pronounced for thicker-shell QDs. Because the QDs used in this work have a relative thick shell with an average particle size of 12–13 nm, the field-induced PL decrease would be quite big and is assumed as the major factor in this case. Owing to the limited preparation conditions, the operational lifetime at a display-relevant luminance of 100 cd m⁻² for device A is ~ 47.4 h (Figure S7). The operational lifetime could be further improved by avoiding exposure to the air, optimization of thick-shell QD structure and EL performance, and better encapsulation method of devices. CIE properties of QLEDs are shown in Figure 4e. The blue EL emission with a narrow FWHM of 20 nm corresponds to CIE 1931 color coordinates of (0.136, 0.078), which is very close to the NTSC 1953 standard of (0.14, 0.08). The color saturation property makes this blue QLED an ideal blue light source for display application. An image of device A at a driving voltage of

Table 1. Summary of Peak Wavelength (λ_{\max}) and FWHM of EL Spectra, CIE, Maximum Luminance (L_{\max}), Maximum CE (CE_{\max}), Maximum EQE (EQE_{\max}), and CE and EQE at Luminance of 1000 cd m⁻²

device	EL λ_{\max} (nm)	FWHM (nm)	CIE 1931	L_{\max} (cd m ⁻²)	CE (cd A ⁻¹)		EQE (%)	
					CE_{\max}	1000 cd m ⁻²	EQE_{\max}	1000 cd m ⁻²
A	468	20	(0.136, 0.078)	4890	14.1	12.5	19.8	17.5
B	468	20	(0.135, 0.077)	2250	9.69	6.08	13.6	8.42
C	464	20	(0.147, 0.068)	3990	8.48	6.08	11.9	8.59
D	464	20	(0.145, 0.068)	3480	4.86	3.86	6.82	5.41

7 V is shown in Figure 4f. Detailed EL characteristics are summarized in Table 1.

CONCLUSION

In summary, we have designed and fabricated pure blue organic–inorganic hybrid structure QLEDs by using thick-shell and high PL QY QDs as the emitting layer, which has suppressed FRET and AR nonradiative progress. We found that small-size ZnO NPs synthesized under a step-controlled mixing process have high electron mobility and smooth surface roughness, and they play a significant role in determining the EL performance. Better charge balance can be realized in blue QLEDs by using PVK as HTL and ZnO NPs as ETL, respectively. As a result, the best performance device has reached a record EQE as high as 19.8% and a maximum CE of 14.1 cd A⁻¹. The CIE 1931 color coordinates (0.136, 0.078) of this device are quite close to the NTSC 1953 standard of (0.14, 0.08). Similar CIE 1931 color coordinates were also obtained for other blue QLEDs with EL peak emission at 464 nm. The color saturation blue QLEDs show great promise for use in next-generation full-color displays. Although the turn-on voltage is higher than the previously reported results^{11,28} due to the usage of thick-shell QDs, we believe that this work offers an effective approach to the realization of high EL efficiency for other color QLEDs, along with transparent and flexible devices.

ASSOCIATED CONTENT

Supporting Information

The Supporting Information is available free of charge on the ACS Publications website at DOI: 10.1021/acsami.7b10785.

Experimental section; TEM images and particle size of QDs; XRD patterns of ZnO NPs and bulk ZnO; PL spectra of ZnO NPs and QDs/ZnO NPs; current density–voltage characteristic of electron-only device; UV-abs and UPS spectra of PVK; lifetime of device; fitted result of PL exponential decay of QDs (PDF)

AUTHOR INFORMATION

Corresponding Authors

*E-mail: linj@ciomp.ac.cn (J. L.).

*E-mail: zhaojl@ciomp.ac.cn (J. Z.).

*E-mail: liuxy@ciomp.ac.cn (X. L.).

ORCID

Jie Lin: 0000-0001-9676-2218

Yongsheng Hu: 0000-0002-8116-4378

Xiaoyang Guo: 0000-0003-0259-137X

Ying Lv: 0000-0003-1649-5258

Jialong Zhao: 0000-0001-9020-1436

Xingyuan Liu: 0000-0002-9681-1646

Notes

The authors declare no competing financial interest.

ACKNOWLEDGMENTS

This work was supported by the CAS Innovation Program, National Natural Science Foundation of China (51503196, 61405195, and 11274304), the Jilin Province Science and Technology Research Projects (20160520176JH, 20160520092JH, and 20150101039JC), and State Key Laboratory of Luminescence and Applications.

REFERENCES

- (1) Dai, X.; Zhang, Z.; Jin, Y.; Niu, Y.; Cao, H.; Liang, X.; Chen, L.; Wang, J.; Peng, X. Solution-Processed, High-Performance Light-Emitting Diodes Based on Quantum Dots. *Nature* **2014**, *515*, 96–99.
- (2) Dong, Y.; Caruge, J. M.; Zhou, Z.; Hamilton, C.; Popovic, Z.; Ho, J.; Stevenson, M.; Liu, G.; Bulovic, V.; Bawendi, M.; Kazlas, P. T.; Steckel, J.; Sullivan, S. C. 20.2: Ultra-Bright, Highly Efficient, Low Roll-Off Inverted Quantum-Dot Light Emitting Devices (QLEDs). *Dig. Tech. Pap. - Soc. Inf. Disp. Int. Symp.* **2015**, *46*, 270–273.
- (3) Manders, J. R.; Qian, L.; Titov, A.; Hyvonen, J.; Tokarz-Scott, J.; Xue, J.; Holloway, P. H. In 8.3: Distinguished Paper: Next-Generation Display Technology: Quantum-Dot LEDs. *Dig. Tech. Pap. - Soc. Inf. Disp. Int. Symp.* **2015**, *46*, 73–75.
- (4) Tan, Z.; Zhang, F.; Zhu, T.; Xu, J.; Wang, A. Y.; Dixon, J. D.; Li, L.; Zhang, Q.; Mohny, S. E.; Ruzyllo, J. Bright and Color-Saturated Emission From Blue Light-Emitting Diodes Based on Solution-Processed Colloidal Nanocrystal Quantum Dots. *Nano Lett.* **2007**, *7*, 3803–3807.
- (5) Shen, H.; Wang, S.; Wang, H.; Niu, J.; Qian, L.; Yang, Y.; Titov, A.; Hyvonen, J.; Zheng, Y.; Li, L. S. Highly Efficient Blue-Green Quantum Dot Light-Emitting Diodes Using Stable Low-Cadmium Quaternary-Alloy ZnCdSSe/ZnS Core/shell Nanocrystals. *ACS Appl. Mater. Interfaces* **2013**, *5*, 4260–4265.
- (6) Shen, H.; Cao, W.; Shewmon, N. T.; Yang, C.; Li, L. S.; Xue, J. High-Efficiency, Low Turn-on Voltage Blue-Violet Quantum-Dot-Based Light-Emitting Diodes. *Nano Lett.* **2015**, *15*, 1211–1216.
- (7) Wang, A.; Shen, H.; Zang, S.; Lin, Q.; Wang, H.; Qian, L.; Niu, J.; Song, L. L. Bright, Efficient, and Color-Stable Violet ZnSe-Based Quantum Dot Light-Emitting Diodes. *Nanoscale* **2015**, *7*, 2951–2959.
- (8) Yang, Y.; Zheng, Y.; Cao, W.; Titov, A.; Hyvonen, J.; Manders, J. R.; Xue, J.; Holloway, P. H.; Qian, L. High-Efficiency Light-Emitting Devices Based on Quantum Dots with Tailored Nanostructures. *Nat. Photonics* **2015**, *9*, 259–266.
- (9) Chen, F.; Lin, Q.; Wang, H.; Wang, L.; Zhang, F.; Du, Z.; Shen, H.; Li, L. S. Enhanced Performance of Quantum Dot-Based Light-Emitting Diodes with Gold Nanoparticle-Doped Hole Injection Layer. *Nanoscale Res. Lett.* **2016**, *11*, 376–384.
- (10) Lin, Q.; Shen, H.; Wang, H.; Wang, A.; Niu, J.; Qian, L.; Guo, F.; Li, L. S. Cadmium-Free Quantum Dots Based Violet Light-Emitting Diodes: High-Efficiency and Brightness via Optimization of Organic Hole Transport Layers. *Org. Electron.* **2015**, *25*, 178–183.
- (11) Kwak, J.; Bae, W. K.; Lee, D.; Park, I.; Lim, J.; Park, M.; Cho, H.; Woo, H.; Yoon, D. Y.; Char, K.; Lee, S.; Lee, C. Bright and Efficient Full-Color Colloidal Quantum Dot Light-Emitting Diodes Using an Inverted Device Structure. *Nano Lett.* **2012**, *12*, 2362–2366.
- (12) Kwak, J.; Lim, J.; Park, M.; Lee, S.; Char, K.; Lee, C. High-Power Genuine Ultraviolet Light-Emitting Diodes Based on Colloidal Nanocrystal Quantum Dots. *Nano Lett.* **2015**, *15*, 3793–3799.

- (13) Shen, H.; Lin, Q.; Cao, W.; Yang, C.; Shewmon, N. T.; Wang, H.; Niu, J.; Li, L. S.; Xue, J. Efficient and Long-Lifetime Full-Color Light-Emitting Diodes Using High Luminescence Yield Thick-Shell Quantum Dots. *Nanoscale* **2017**, *9*, 13583–13591.
- (14) Ji, W.; Wang, T.; Zhu, B.; Zhang, H.; Wang, R.; Zhang, D.; Chen, L.; Yang, Q.; Zhang, H. Highly Efficient Flexible Quantum-Dot Light Emitting Diodes With an ITO/Ag/ITO Cathode. *J. Mater. Chem. C* **2017**, *5*, 4543–4548.
- (15) Shirasaki, Y.; Supran, G. J.; Bawendi, M. G.; Bulović, V. Emergence of Colloidal Quantum-Dot Light-Emitting Technologies. *Nat. Photonics* **2012**, *7*, 13–23.
- (16) Rogach, A. L.; Klar, T. A.; Lupton, J. M.; Meijerink, A.; Feldmann, J. Energy Transfer with Semiconductor Nanocrystals. *J. Mater. Chem.* **2009**, *19*, 1208–1221.
- (17) Lee, K. H.; Lee, J. H.; Kang, H. D.; Park, B.; Kwon, Y.; Ko, H.; Lee, C.; Lee, J.; Yang, H. Over 40 cd/A Efficient Green Quantum Dot Electroluminescent Device Comprising Uniquely Large-Sized Quantum Dots. *ACS Nano* **2014**, *8*, 4893–4901.
- (18) Garcia-Santamaria, F.; Brovelli, S.; Viswanatha, R.; Hollingsworth, J. A.; Htoon, H.; Crooker, S. A.; Klimov, V. I. Breakdown of Volume Scaling in Auger Recombination in CdSe/CdS Heteronanocrystals: The Role of the Core-Shell Interface. *Nano Lett.* **2011**, *11*, 687–693.
- (19) Kim, H. M.; Kim, J.; Lee, J.; Jang, J. Inverted Quantum-Dot Light Emitting Diode Using Solution Processed p-Type WO_x Doped PEDOT:PSS and Li Doped ZnO Charge Generation Layer. *ACS Appl. Mater. Interfaces* **2015**, *7*, 24592–24600.
- (20) Cao, S.; Zheng, J.; Zhao, J.; Yang, Z.; Li, C.; Guan, X.; Yang, W.; Shang, M.; Wu, T. Enhancing the Performance of Quantum Dot Light-Emitting Diodes Using Room-Temperature-Processed Ga-Doped ZnO Nanoparticles as the Electron Transport Layer. *ACS Appl. Mater. Interfaces* **2017**, *9*, 15605–15614.
- (21) Pan, J.; Chen, J.; Huang, Q.; Khan, Q.; Liu, X.; Tao, Z.; Zhang, Z.; Lei, W.; Nathan, A. Size Tunable ZnO Nanoparticles to Enhance Electron Injection in Solution Processed QLEDs. *ACS Photonics* **2016**, *3*, 215–222.
- (22) Liang, X.; Bai, S.; Wang, X.; Dai, X.; Gao, F.; Sun, B.; Ning, Z.; Ye, Z.; Jin, Y. Colloidal Metal Oxide Nanocrystals As Charge Transporting Layers for Solution-Processed Light-Emitting Diodes and Solar Cells. *Chem. Soc. Rev.* **2017**, *46*, 1730–1759.
- (23) Sun, Q.; Wang, Y. A.; Li, L. S.; Wang, D.; Zhu, T.; Xu, J.; Yang, C.; Li, Y. Bright, Multicoloured Light-Emitting Diodes Based on Quantum Dots. *Nat. Photonics* **2007**, *1*, 717–722.
- (24) Shen, H.; Bai, X.; Wang, A.; Wang, H.; Qian, L.; Yang, Y.; Titov, A.; Hyvonen, J.; Zheng, Y.; Li, L. S. High-Efficient Deep-Blue Light-Emitting Diodes by Using High Quality Zn_xCd_{1-x}S/ZnS Core/Shell Quantum Dots. *Adv. Funct. Mater.* **2014**, *24*, 2367–2373.
- (25) Anikeeva, P. O.; Halpert, J. E.; Bawendi, M. G.; Bulovic, V. Quantum Dot Light-Emitting Devices with Electroluminescence Tunable over the Entire Visible Spectrum. *Nano Lett.* **2009**, *9*, 2532–2536.
- (26) Shirasaki, Y.; Supran, G. J.; Tisdale, W. A.; Bulović, V. Origin of Efficiency Roll-Off in Colloidal Quantum-Dot Light-Emitting Diodes. *Phys. Rev. Lett.* **2013**, *110*, 217403.
- (27) Bozyigit, D.; Yarema, O.; Wood, V. Origins of Low Quantum Efficiencies in Quantum Dot LEDs. *Adv. Funct. Mater.* **2013**, *23*, 3024–3029.
- (28) Qian, L.; Zheng, Y.; Xue, J.; Holloway, P. H. Stable and Efficient Quantum-Dot Light-Emitting Diodes Based on Solution-Processed Multilayer Structures. *Nat. Photonics* **2011**, *5*, 543–548.